Hindawi
Advances in Materials Science and Engineering
Volume 2018, Article ID 1437069, 9 pages
https://doi.org/10.1155/2018/1437069

Research Article

Influence of Macrotexture and Microtexture on the Skid Resistance of Aggregates

Bowen Guan [1], Jiayu Wu [1], Chao Xie [1], Jianhong Fang [2], Haile Zheng [3], and Huaxin Chen [1]

[1] *School of Material Science and Engineering, Chang'an University, Xi'an, Shaanxi 710064, China*
[2] *Qinghai Research Institute of Transportation, Xining, Qinghai 810008, China*
[3] *The 2ND Engineering CO, LTD of China Railway 17 Bureau Group Corporation, Xi'an, Shaanxi 710064, China*

Correspondence should be addressed to Huaxin Chen; chenhx_paper@163.com

Received 15 May 2018; Revised 3 September 2018; Accepted 6 September 2018; Published 18 October 2018

Guest Editor: Ghazi G. Al-Khateeb

This article intends to study the influence of macrotexture and microtexture on the skid resistance of four types of aggregates. For this purpose, fractal dimension (D), root mean square height (R_q), and Polished Stone Value (PSV) were tested. The Pearson correlation coefficients between PSV and D or R_q in the interval of different polishing cycles were calculated and analyzed with correlation analysis. The relationships between PSV and R_q were also established. The results showed that the PSV development was approximately divided into 3 stages including accelerated attenuation stage, decelerated attenuation stage, and stabilization stage. There is a critical point of the entire polishing cycles. When the number of the polishing cycles exceeds this critical point, microtexture replaces macrotexture to play a major role in the skid resistance of aggregates. In the accelerated attenuation stage, macrotexture plays a major role in the skid resistance of aggregates. In the decelerated attenuation stage and stabilization stage, microtexture gradually plays a major role in the skid resistance of aggregates. Because of roughest microtexture in the stabilization stage, bauxite can provide the highest levels of skid resistance for high friction surface treatment over the long-term period.

1. Introduction

High friction surface treatment (HFST) is the application of very high quality aggregate with an epoxy binder, which is designed to improve friction of the pavement in the location with high crashes, such as horizontal curves and intersections. As an approach widely used in the pavement construction and maintenance, HFST has been demonstrated to provide significant increases in friction [1–3].

Due to surface texture characteristics directly affecting the skid resistance of the pavement, lots of researchers focus on the influence of surface texture on the skid resistance of HFST. Heitzman et al. [4] evaluated the HFST test slabs with eight aggregates including bauxite, granite, flint, basalt, silica sand, steel slag, emery, and taconite under accelerated laboratory polishing and testing procedures. They found that all eight surfaces maintained predominately greater than 1.0 mm mean profile depth (MPD), and however, there is no correlation between HFST surface friction and particle shape and angularity. Li et al. [5] reported that friction surfacing such as HFST with larger surface MPD does not necessarily produce greater surface friction. Chen et al. [6] put forward that the surface of the coarse aggregate tended to have a smooth microstructure due to the reducing actual effective contact area of the road surface greatly. Even if with the same macrostructure depth of the road surface, the skid resistance ability of the road surface would be also decreased. Most of the studies have found that not only macrotexture varies with aggregate geometric properties (shape and size) but also microtexture has significant influence on the skid resistance of HFST. However, their effects have not been quantified.

Because aggregate in the pavement materials accounts for more than 90%, surface texture of aggregate is important for friction of HFST. The appearance of aggregates is mainly divided into two levels: macrotexture and microtexture. The first level is characterized by a shape that reflects the change in the size of a particle, that is, the macroscopic overall variation of the aggregate particles and the state. The second level is characterized by texture used to describe the surface of a body in an irregular range. The impact of texture is often so small which cannot affect the shape or edges and corners, reflecting the aggregate particles microscopic-scale changes within the scope of the situation. In order to understand the relationship between surface texture and skid resistance of aggregates, the effect of macrotexture and microtexture was quantified, and their contributions to the skid resistance of aggregates were studied in this paper.

2. Materials and Methods

2.1. Raw Materials. Four types of aggregates (bauxite, granite, limestone, and basalt) were used in this research. The bauxite, used for antiwear purposes in pavement engineering, was calcined to 1600°C, which is commonly used in HFST [7]. The alternative aggregates granite and basalt were also selected. Limestone was chosen as a control group, which is commonly used in wear course. The bauxite samples were obtained from Yangquan city, China. The other aggregates samples were obtained from Xi'an city, China. Aiming at measurement of surface morphology and antipolishing, these four types of aggregates were determined with different test methods on grains with a size of 9.5/13.2 mm.

2.2. Experimental Method

2.2.1. PSV Test. As the key factor in estimating the quality of aggregates used for HFST, Polished Stone Value (PSV) was used to evaluate the friction resistance of aggregate. The PSV test was carried out according to the Chinese standard JTG E42-2005 [8]. Samples of coarse aggregate were mixed up in resin to form the specimens which were coupled onto the circumference of a wheel in an accelerated polishing machine. Fourteen specimens were clamped around the periphery of the wheel and subjected to two phases of polishing by wheels with rubber tyres. To eliminate the effect of the aggregate manufacturing process on the microtexture of aggregate, the preparatory phase was of abrasion by corn emery for 40000 cycles. The polishing action was carried out with a velocity of 320 ± 5 r/min and with a load of 725 ± 10 N. Then, 40000, 80000, 120000,160000, 200000, 240000, and 280000 cycles of polishing with emery flour were followed. The degree of polish of the specimens was then measured by means of the British Pendulum device. Results were expressed as Polished Stone Value (PSV), the mean of the fourteen test specimens of each aggregate.

2.2.2. Macrotexture Measurement. Fractal dimension is an index for characterizing fractal patterns or sets by quantifying their complexity as a ratio of the change in detail to the change in scale. Many researchers have found that fractal dimension is the suitable parameter for characterizing a pavement surface, and it is an effective measure to describe shape and angularity of the surface [9, 10]. With increasing complexity or surface roughness, the fractal dimension increases [11]. For the purpose of obtaining the macrotexture characteristics of aggregate, the images of the specimens in different polishing cycles were collected by the Sony DSC-RX100M2 digital camera. The resolution of the images was 200 μm. A red-green-blue (RGB) image was converted to grayscale first. The images can be considered as a 3D space, in which the two coordinates (X, Y) represent the 2D position and the third coordinate I represents the image grey level intensity. Then, image data were converted to a numeric array, and box-counting dimension (D) was calculated by MATLAB software.

2.2.3. Microtexture Measurement. 3D color laser microscope system was mainly used for 3D surface analysis and characterization. The laser is used to scan the surface in the *XYZ* directions and collect data throughout the entirety of a specified range. The result is a high-resolution, large depth-of-field, color image with nanometer-level height resolution for accurate profile and roughness measurements [12, 13]. As shown in Figure 1, the 3D color laser microscope system which was produced by Keyence Inc was used to measure and calculate the root-mean square height of four aggregates in this work. To reduce the acquisition error of the microscopic test data, five surfaces of aggregates on a polished specimen were observed. According to the BS EN ISO 4287: 2000 standard, the surface texture parameter (the root-mean square height R_q) was obtained by the VK-Analyzer [14]. VK-Analyzer is the software module which complies with ISO 25178 and allows users to complete measurements of several surface parameters.

3. Results and Discussions

3.1. Variation of PSV during the Long-Term Polishing Process. Figure 2 showed that the four types of aggregates exhibited approximately the same PSV development trend.

From Figure 2, it can be seen that the value of PSV decreases with the increase of polishing cycles. The attenuation rate of PSV increased first and then decreased. After the polishing cycles reached a certain value, the value of PSV stayed roughly the same. In order to distinguish the inflection point of increase and decrease of attenuation rate of PSV, the second-order differential results of the PSV curves are obtained by using Origin software dealing with the PSV curves. Differential results of the PSV curves can show the change rate of attenuation rate of PSV, which is described in Figure 3.

From Figure 3, it can be seen that the change rate of attenuation rate of PSV increases first and then decreases with the increase of the polishing cycles. The peak point was the inflection point of increase and decrease of attenuation rate of PSV. When attenuation rate of PSV was first close to 0, the point was the inflection point of decrease and steady of attenuation rate of PSV. The PSV development was approximately divided into 3 stages including the accelerated attenuation stage, decelerated attenuation stage, and stabilization stage.

In the PSV test, different types of aggregates exhibit different skid resistance during the long-term polishing

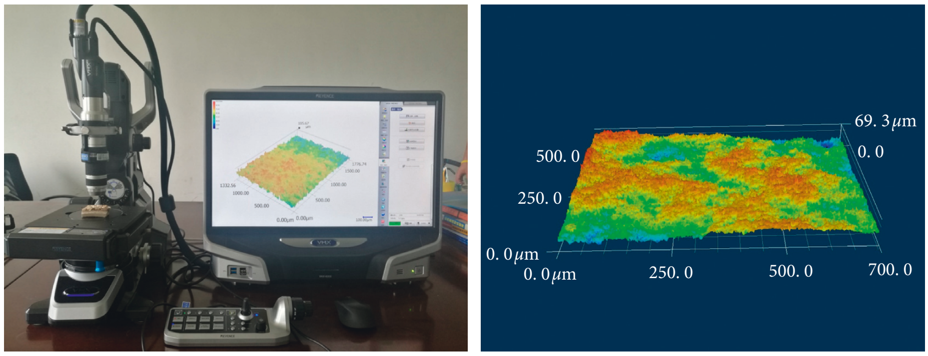

FIGURE 1: Illustration of 3D laser microscopy measurement.

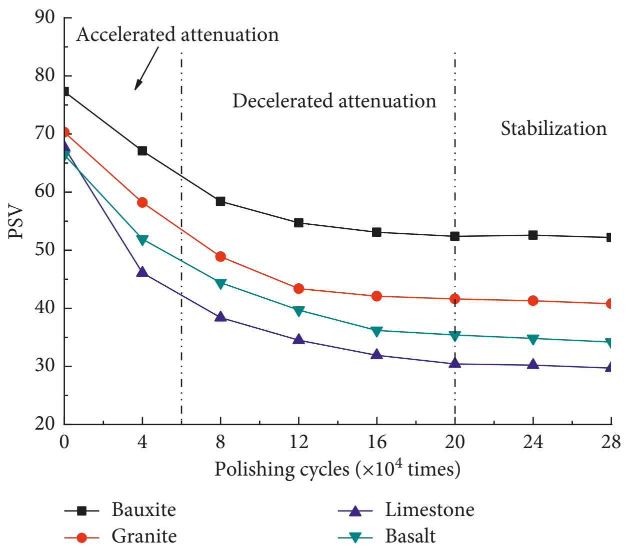

FIGURE 2: Variation of PSV during the long-term polishing process.

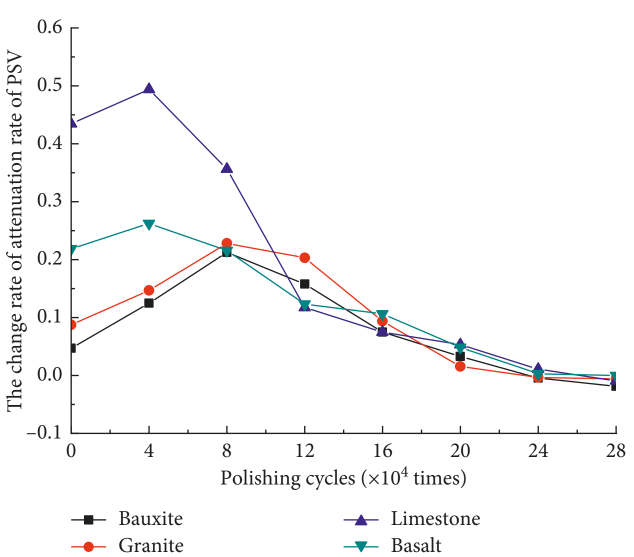

FIGURE 3: Second-order differential PSV curves.

process. The value of PSV of bauxite was decreased by 32%, and the final value of PSV was around 52. Skid resistance of bauxite was maintained at a relatively high level. Granite and basalt ranked second and third, respectively. Limestone has the lowest value of PSV in the stabilization stage. Therefore, bauxite was more suitable for the wearing course, especially high friction surface treatment.

3.2. Variation of D and R_q during the Long-Term Polishing Process. Figure 4 presents variation of *D* during the long-term polishing process. *D* is calculated by image analysis. The images are obtained by a digital camera, and the resolution of the images is 200 μm. This test method meets the accuracy requirements for testing macrotexture.

As seen from Figure 4, the value of *D* decreases with the increase of polishing cycles. When the polishing cycles reach 240,000 times, the values of *D* of different aggregates are similar. Figure 5 shows the change of macrotexture after the long-term polishing process.

From Figure 5, it can be seen that the angularity of the aggregate surface is polished, and the macrotexture of aggregates become smooth and were difficult to distinguish. Therefore, the value of *D* in the stabilization stage is similar; that is, the macrotexture of different aggregates is similar.

Figure 6 presents variation of R_q during the long-term polishing process. R_q is obtained by the 3D color laser microscope system. The 3D color laser microscope system is a laser scanning microscope to perform noncontact 3D observations and measurements of surface features at 10 nanometer resolutions. This equipment meets the accuracy requirements for testing microtexture.

From Figure 6, it can be seen that the R_q curve is similar to the PSV curve. The value of R_q decreases with the increase of polishing cycles. Figures 7–10 display the change of micromorphology of surface of different aggregates before and after the polishing process.

From Figures 7–10, it can be found that the mineral on the aggregate surface was first destroyed rapidly, and it was peeled off from the surface of aggregate or become powder filled in pores. The surface microtexture is destroyed by the external friction obviously, and the surfaces of aggregates become smooth. After the polishing cycles reach a certain time, the value of R_q stayed roughly the same. The R_q development was approximately divided into 2 stages including the attenuation stage of microtexture and the stabilization stage of microtexture. Figure 11 is a schematic

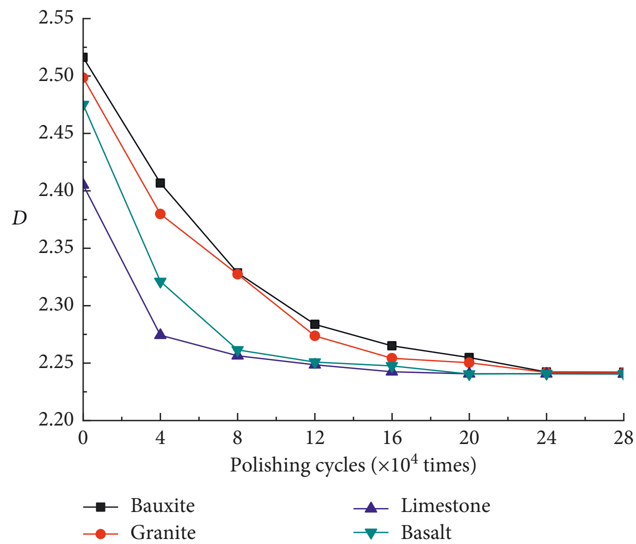

Figure 4: Variation of D during the long-term polishing process.

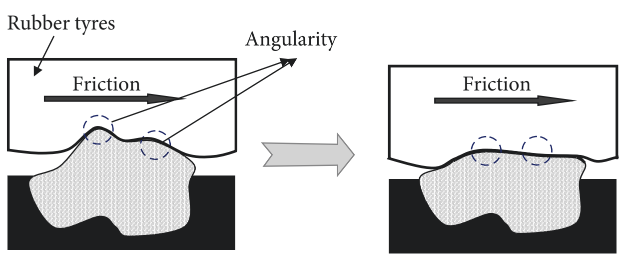

Figure 5: The change of macrotexture after the long-term polishing process.

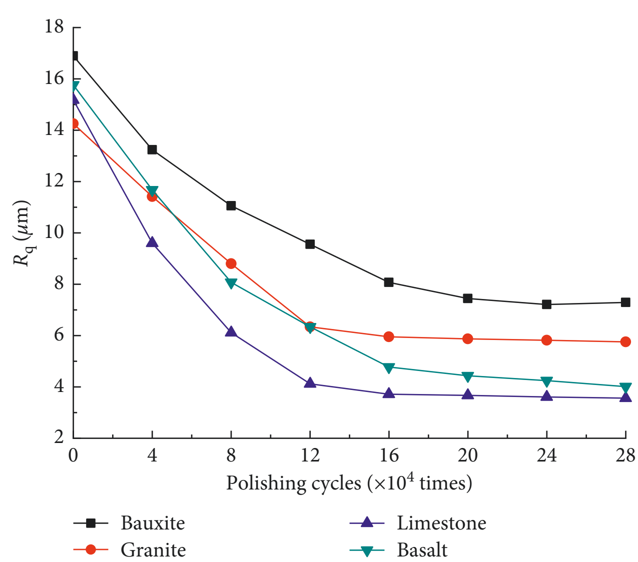

Figure 6: Variation of R_q during the long-term polishing process.

diagram of microtexture change during the long-term polishing process.

According the value of R_q of different aggregates after the long-term polishing process, bauxite can provide the roughest surface against external forces. Granite and basalt ranked second and third, respectively. Limestone has the smoothest surface and has the lowest value of R_q. Due to different mineral compositions, the final microtexture of different aggregates is different. The main mineral composition of limestone is calcite and dolomite. The Mohs hardness of the two minerals are similar (3~4) [15]. The mineral particles are soft and easy to be polished. Therefore, the microtexture of limestone is smoother than the other aggregates. The main crystal phase of bauxite is composed of corundum and mullite. The Mohs hardness of corundum and mullite are 9 and 6.5, respectively [15]. The mineral particles are hard and difficult to be polished. This is the reason why the microtexture of the bauxite surface is roughest and has good ability to resist the damage of external friction.

3.3. The Correlation between PSV and D or R_q. According to the above analysis, the macrotexture and the microtexture of aggregates affect the value of PSV of aggregates together. However, the degree of influence is different. In order to analyze the difference in the degree of influence, the correlation coefficient between PSV and D or R_q in the interval of different polishing cycles were calculated with Pearson correlation analysis. The results are shown in Figures 12 and 13.

From Figures 12 and 13, it can be seen that the Pearson correlation coefficient between D and PSV is higher than the Pearson correlation coefficient between R_q and PSV in the early stage of the polishing process, and the macrotexture has a greater influence on PSV. With the increase of the polishing cycles, the Pearson correlation coefficient between D and PSV decreases, and the degree of influence of macrotexture on skid resistance of aggregates becomes smaller. While the Pearson correlation coefficient between R_q and PSV increases, the degree of influence of microtexture becomes larger. The microtexture has the larger degree of influence on PSV in the late stage of the polishing process. It can be inferred that there is a critical point of the polishing cycles, and when the number of the polishing cycles exceed this point, microtexture will replace macrotexture to play a major role in the skid resistance of aggregates.

In order to find out the critical point, 4×10^4, 8×10^4, 12×10^4, 16×10^4, and 20×10^4 polishing cycles are assumed to be demarcation points, respectively. The Pearson correlation coefficients of PSV and D in the front interval ($0{\sim}4 \times 10^4$, $0{\sim}8 \times 10^4$, $0{\sim}12 \times 10^4$, $0{\sim}16 \times 10^4$, and $0{\sim}20 \times 10^4$ times) and the Pearson correlation coefficients of PSV and R_q in the after interval ($4 \times 10^4{\sim}28 \times 10^4$, $8 \times 10^4{\sim}28 \times 10^4$, $12 \times 10^4{\sim}28 \times 10^4$, $16 \times 10^4{\sim}28 \times 10^4$ and $20 \times 10^4{\sim}28 \times 10^4$ times) are calculated, which are shown in Figure 14.

From Figure 14, it can be found that when 4×10^4 times is selected as the demarcation point, the Pearson correlation coefficients of PSV and D in the front interval ($0{\sim}4 \times 10^4$ times) is higher than the Pearson correlation coefficients of PSV and R_q in the after interval ($4 \times 10^4 \sim 28 \times 10^4$ times). Macrotexture plays a major role in the skid resistance of aggregates. When 8×10^4 times is selected as the

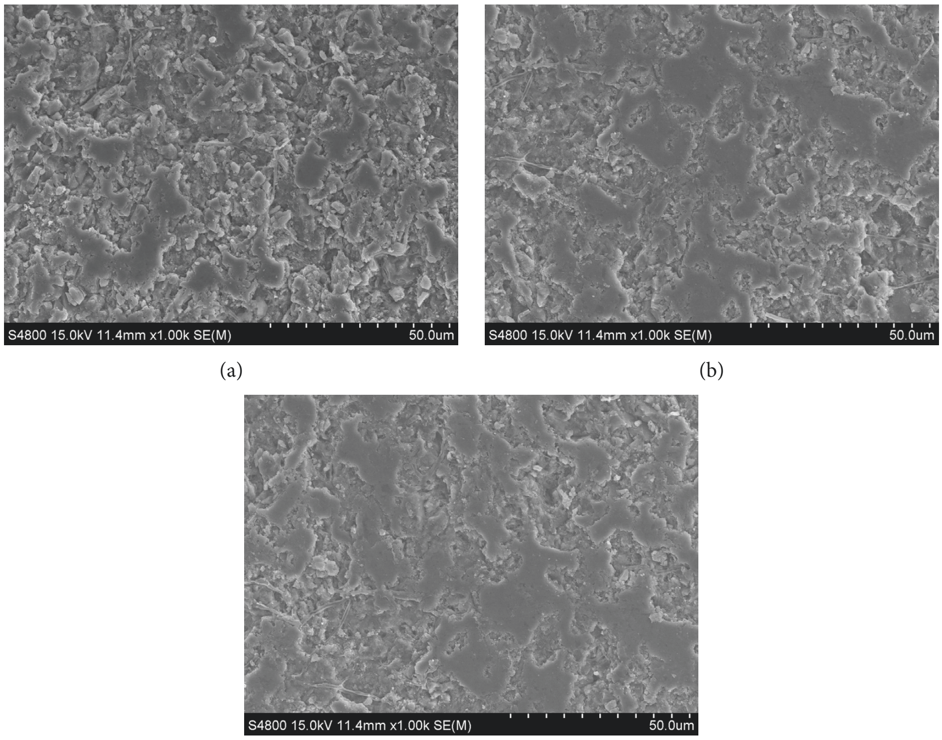

(a) (b)

(c)

Figure 7: Micromorphology of the bauxite surface: (a) before the polishing process; (b) after 20×10^4 polishing cycles; (c) after 28×10^4 polishing cycles.

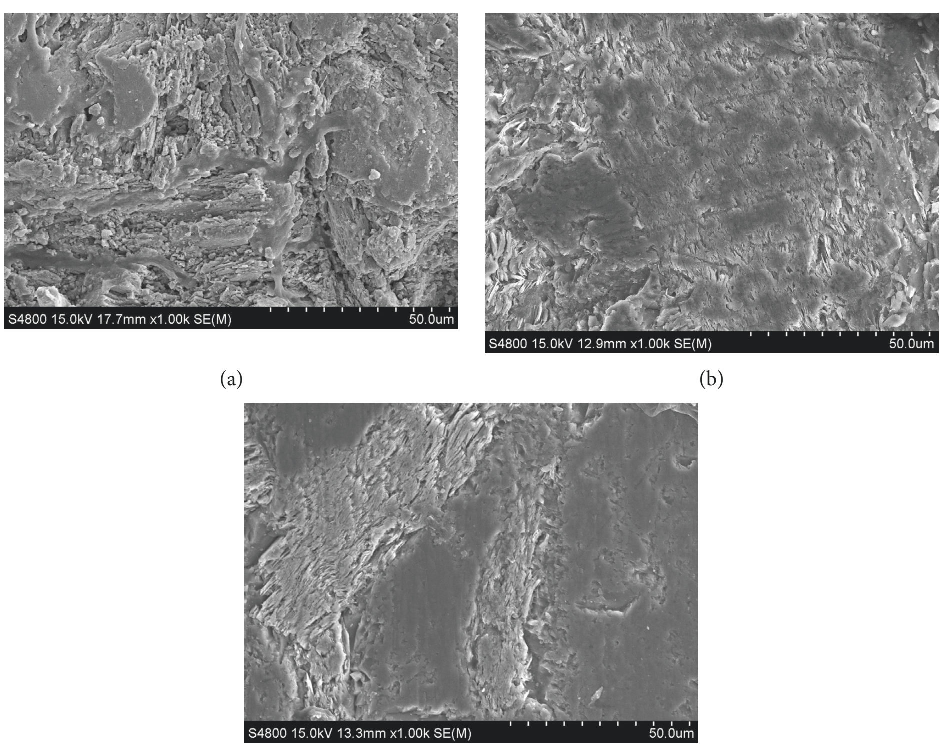

(a) (b)

(c)

Figure 8: Micromorphology of the granite surface: (a) before the polishing process; (b) after 20×10^4 polishing cycles; (c) after 28×10^4 polishing cycles.

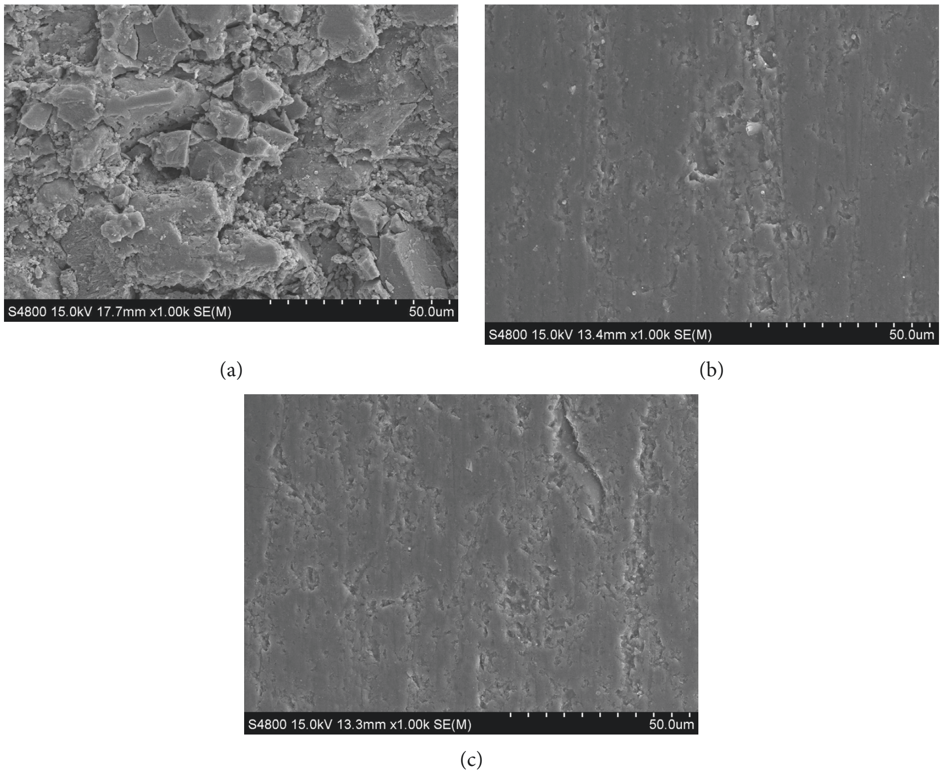

Figure 9: Micromorphology of the limestone surface: (a) before the polishing process; (b) after 20×10^4 polishing cycles; (c) after 28×10^4 polishing cycles.

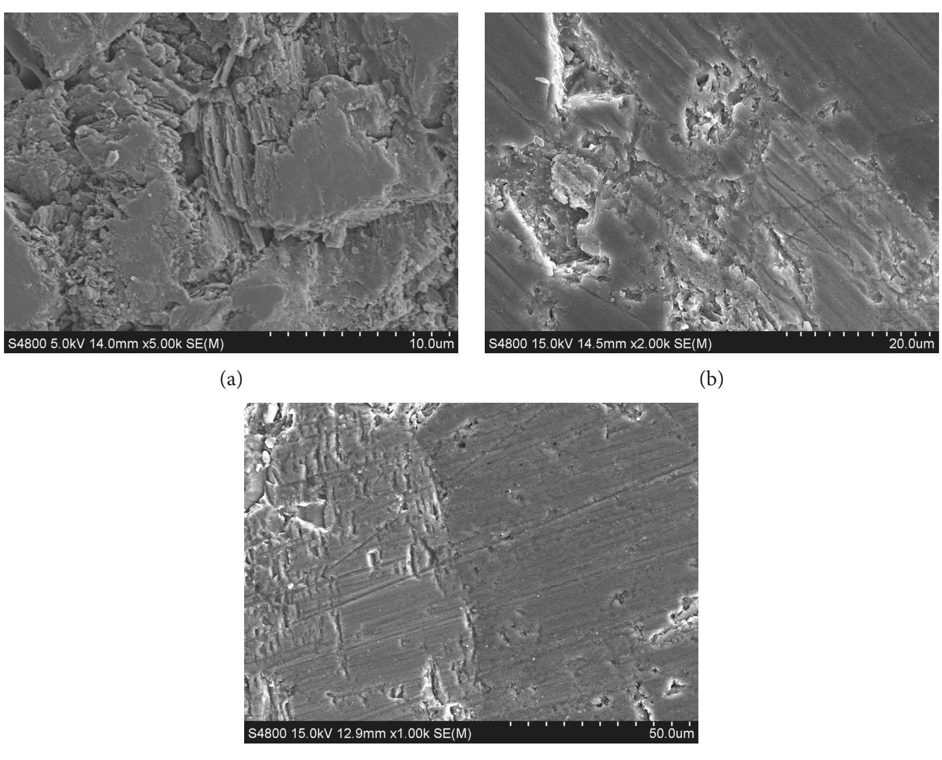

Figure 10: Micromorphology of the basalt surface: (a) before the polishing process; (b) after 20×10^4 polishing cycles; (c) after 28×10^4 polishing cycles.

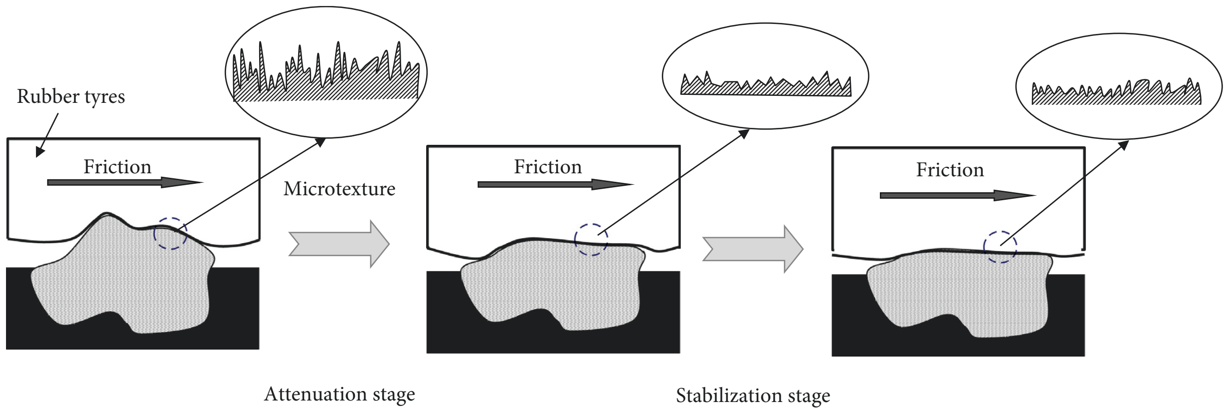

FIGURE 11: Schematic diagram of microtexture change during the long-term polishing process.

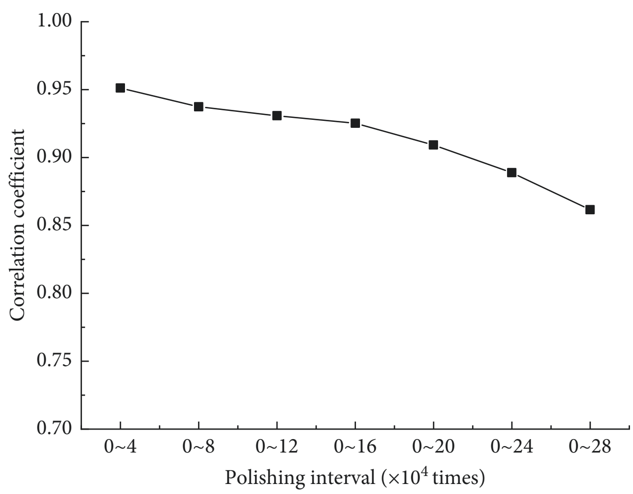

FIGURE 12: Pearson correlation coefficient between PSV and D at different polishing intervals.

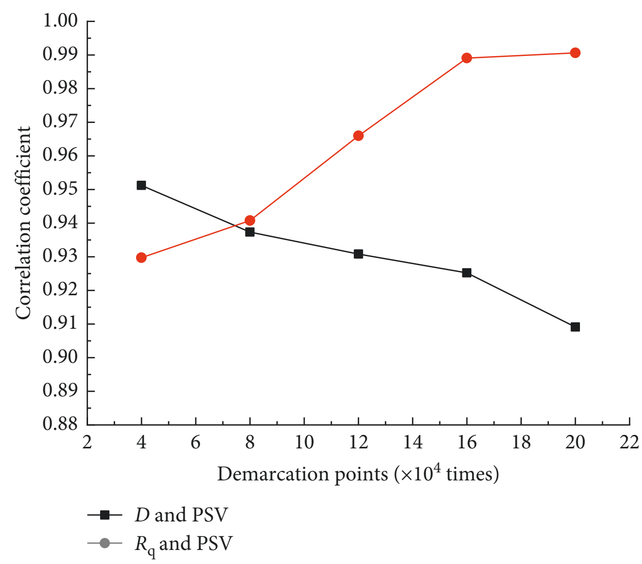

FIGURE 14: The Pearson correlation coefficient between PSV and D or Rq at different demarcation points.

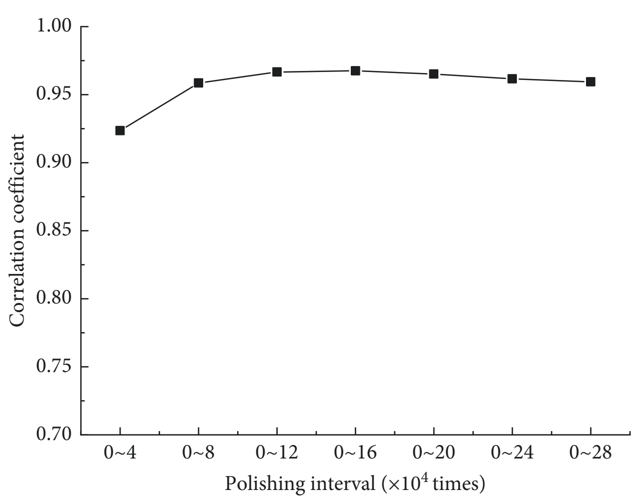

FIGURE 13: Pearson correlation coefficient between PSV and Rq at different polishing intervals.

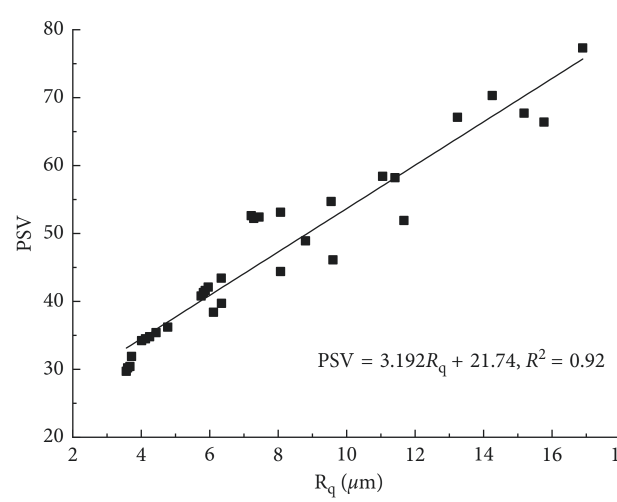

FIGURE 15: Correlation between PSV and R_q.

demarcation point, the Pearson correlation coefficients of PSV and R_q in the after interval (0~8 × 10^4 times) is higher than the Pearson correlation coefficients of PSV and D in the front interval (8 × 10^4~28 × 10^4 times). The microtexture had replaced macrotexture to play a major role in the skid resistance of aggregates. Therefore, the critical point is between 4 × 10^4 times and 8 × 10^4 times.

This point may have a relationship with the inflection point of increase and decrease of attenuation rate of PSV, which is shown in Figure 3. In the accelerated attenuation stage, macrotexture plays a major role in the skid resistance of aggregates. When the aggregate is subjected to friction, the angularity of the aggregates is destroyed, and the value of PSV decreases in acceleration. In the decelerated attenuation stage, microtexture gradually plays a major role in the skid resistance of aggregates. The microtexture is destroyed by the external friction slowly, and the value of PSV decreases in the deceleration stage. In the stabilization stage, under the effect of friction, the mineral crystal gradually emerges, and the microtexture maintains a stable state.

In summary, macrotexture has significant influence on the early skid resistance performance of aggregates, and microtexture has significant influence on the long-term skid resistance performance. Due to the fact that polishing of the aggregate in the pavement is the long-term process, microtexture is more important for long-term skid resistance of aggregates. R_q is a suitable indicator to evaluate the long-term skid resistance of aggregates. The correlations between PSV and R_q were studied by a mathematical fitting, which is illustrated in Figure 15. From Figure 15, it can be seen that the correlation coefficient of the linear-fitted equation is 0.92, which shows the good linear correlation between PSV and R_q.

4. Conclusions

(1) The PSV development is approximately divided into 3 stages including the accelerated attenuation stage, decelerated attenuation stage, and stabilization stage.

(2) There is a critical point in the entire polishing cycles. When the number of the polishing cycles exceeds this critical point, microtexture replaces macrotexture to play a major role in the skid resistance of aggregates.

(3) R_q in the stabilization stage is a suitable indicator to evaluate the long-term skid resistance of aggregates.

(4) Due to the highest value of R_q in the stabilization stage, bauxite had higher skid resistance during the long-term polishing process, and it was suitable for the wearing course, especially high friction surface treatment.

Data Availability

The authors would like to declare that all the data in the manuscript were obtained by experiment, and the data are true and effective in the manuscript.

Conflicts of Interest

The authors declare that they have no conflicts of interest.

Acknowledgments

The authors wish to thank the National Key R&D Program of China (2017YFB0309903), the Qinghai Provincial Natural Science Foundation (2017-ZJ-764), Traffic Construction Project of Science and Technology of Shaanxi Province (16-16K), National Natural Science Foundation of China (51608046), and Special Fund for Scientific Research of Central Colleges, Chang'an University (310831172201, 300102318401, and 300102318501).

References

[1] K. W. Anderson, M. Russell, J. S. Uhlmeyer et al., *Kwik Bond Polymers® High FrictionSurface Treatment*, Washington State Department of Transportation, Olympia, WA, USA, 2015.

[2] Q. J. Li, G. W. Yang, K. C. Wang, Y. Zhan, D. Merritt, and C. Wang, "Effectiveness and performance of high friction surface treatments at a national scale," *Canadian Journal of Civil Engineering*, vol. 43, no. 9, pp. 812–821, 2016.

[3] V. Reddy, T. Datta, P. Savolainen et al., "A study of the effectiveness of tyregrip high friction surface treatment," *Accident Reconstruction Journal*, vol. 19, no. 5, pp. 53–57, 2009.

[4] M. Heitzman, P. Turner, and M. Greer, "High friction surface treatment alternative aggregates study," NCAT Report 15-04, Auburn University, Auburn, AL, Australia, 2015.

[5] S. Li, R. Xiong, D. Yu, G. Zhao, P. Cong, and Y. Jiang, "Friction surface treatment selection: aggregate properties, surface characteristics, alternative treatments and safety effects," Tech. Rep. FHWA/IN/JTRP-2017/09, Purdue University, West Lafayette, IN, USA, 2017.

[6] X. Chen, S. Dai, Y. Guo, J. Yang, and X. Huang, "Polishing of asphalt pavements: from macro-to micro-scale," *Journal of Testing and Evaluation*, vol. 44, no. 2, pp. 885–894, 2015.

[7] S. J. Dews and R. J. Bishop, "Factors affecting the skid-resistance of calcined bauxite," *Journal of Chemical Technology and Biotechnology*, vol. 22, no. 10, pp. 1117–1124, 2010.

[8] JTG E42-2005, *Test Methods of Aggregate for Highway Engineering*, Research Institute of Highway of the Ministry of Communications, Ministry of Communications of the PRC, Beijing, China, 2005.

[9] K. D. Lawrence and B. Ramamoorthy, "Surface texture evaluation of cylinder liners using machine vision," in *Proceedings of the 11th WSEAS International Conference on Electronics, Hardware, Wireless and Optical Communications, and Proceedings of the 11th WSEAS International Conference on Signal Processing, Robotics and Automation, and Proceedings of the 4th WSEAS International Conference on Nanotechnology*, World Scientific and EngineeringAcademy and Society (WSEAS), pp. 143–148, Cambridge, UK, February 2012.

[10] R. A. Boby, M. Hanmandlu, A. Sharma et al., "Extraction of fractal dimension for iris texture," in *Proceedings of Iapr International Conference on Biometrics*, pp. 330–335, New Delhi, India, September 2012.

[11] R. Kumar, P. Kulashekar, B. Dhanasekar, and B. Ramamoorthy, "Application of digital image magnification for surface roughness evaluation using machine vision," *International Journal of Machine Tools and Manufacture*, vol. 45, no. 2, pp. 228–234, 2005.

[12] Z. Qian and L. Meng, “Study on micro-texture and skid resistance of aggregate during polishing,” *Frontiers of Structural and Civil Engineering*, vol. 11, no. 3, pp. 346–352, 2017.

[13] B. K. Abban, A. T. Papanicolaou, C. P. Giannopoulos et al., “Quantifying the changes of soil surface micro roughness due to rainfall impact on a smooth surface,” *Nonlinear Processes in Geophysics*, vol. 24, no. 3, pp. 569–579, 2017.

[14] International Organization for Standardization, *Geometrical Product Specifications (GPS)-surface Texture: Profile Method-terms, Definitions and Surface Texture Parameters*, ISO, Geneva, Switzerland, 1997.

[15] G. V. Samsonov, *Mechanical Properties of the Elements, Handbook of the Physicochemical Properties of the Elements*, Springer, New York, NY, USA, 1968.

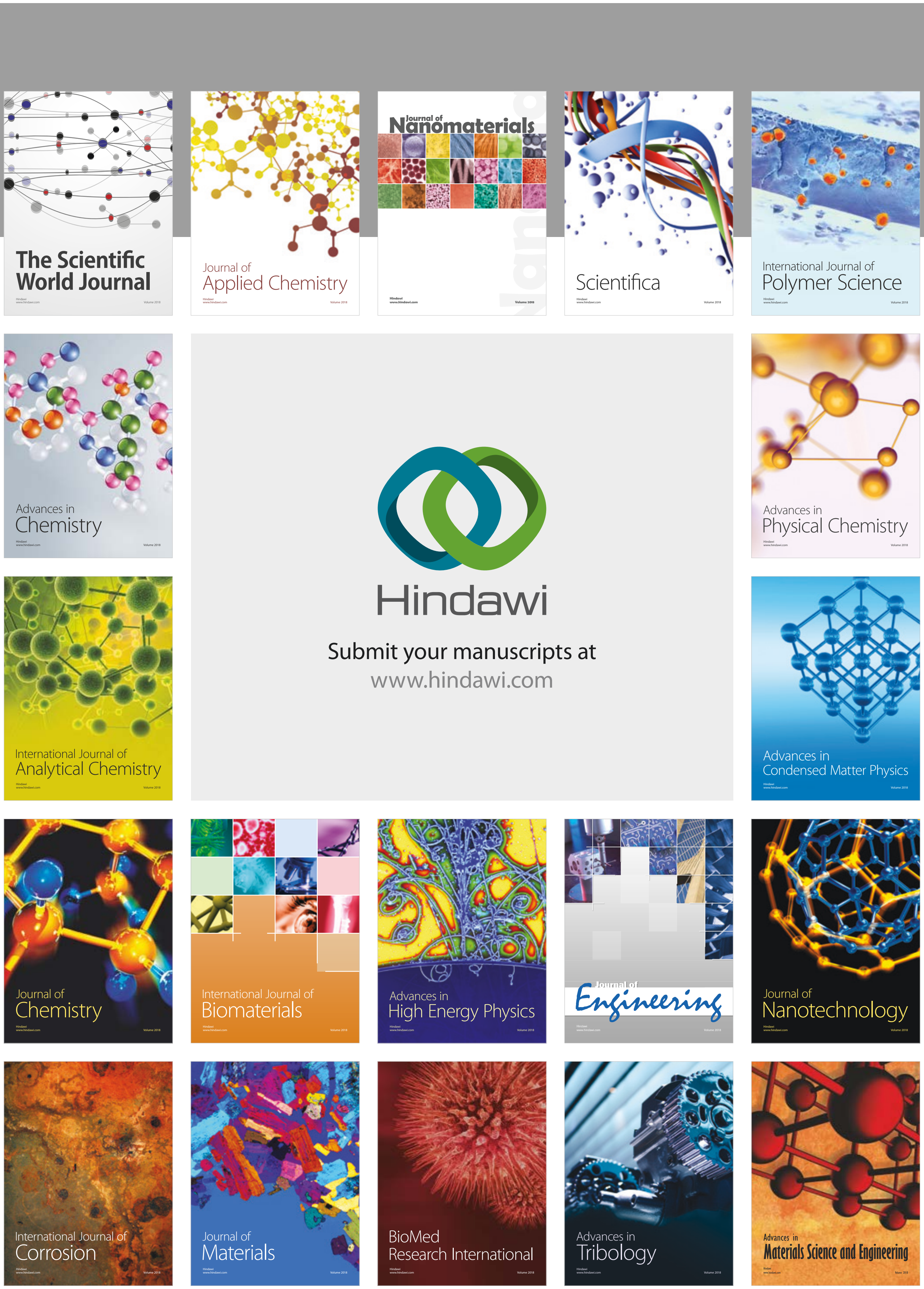

The Scientific World Journal
Journal of Applied Chemistry
Journal of Nanomaterials
Scientifica
International Journal of Polymer Science
Advances in Chemistry
Hindawi
Submit your manuscripts at
www.hindawi.com
Advances in Physical Chemistry
International Journal of Analytical Chemistry
Advances in Condensed Matter Physics
Journal of Chemistry
International Journal of Biomaterials
Advances in High Energy Physics
Journal of Engineering
Journal of Nanotechnology
International Journal of Corrosion
Journal of Materials
BioMed Research International
Advances in Tribology
Advances in Materials Science and Engineering